

Copper-Catalyzed Tyrosine Nitration

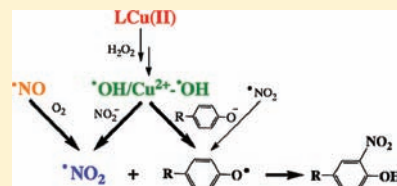
Liang Qiao,[†] Yu Lu,[†] Baohong Liu,[‡] and Hubert H. Girault^{*,†}

[†]Laboratoire d'Electrochimie Physique et Analytique, Ecole Polytechnique Fédérale de Lausanne, Station 6, CH-1015 Lausanne, Switzerland

[‡]Department of Chemistry, Institute of Biomedical Sciences, Fudan University, Shanghai 200433, People's Republic of China

 Supporting Information

ABSTRACT: Tyrosine nitration, often observed during neurodegenerative disorders under nitrative stress, is usually considered to be induced chemically either by nitric oxide and oxygen forming nitrogen dioxide or by the decomposition of peroxynitrite. It can also be induced enzymatically by peroxidases or superoxide dismutases in the presence of both hydrogen peroxide and nitrite forming nitrogen dioxide and/or peroxynitrite. In this study, the role of cupric ions for catalyzing tyrosine nitration in the presence of hydrogen peroxide and nitrite, by a chemical mechanism rather similar to enzymatic pathways where nitrite is oxidized to form nitrogen dioxide, was investigated by development of a microreactor also capable of acting as an emitter for electrospray ionization mass spectrometry analysis. Indeed, cupric ions and peptide–cupric ion complexes are found to be excellent Fenton catalysts, even better than Fe(III) or heme, for the formation of $\cdot\text{OH}$ radicals and/or copper(II)-bound $\cdot\text{OH}$ radicals from hydrogen peroxide. These radicals are efficiently scavenged by nitrite anions to form $\cdot\text{NO}_2$ and by tyrosine to form tyrosine radicals, leading to tyrosine nitration in polypeptides. We also show that cupric ions can catalyze tyrosine nitration from nitric oxide, oxygen, and hydrogen peroxide as the formation of tyrosine radicals is increased in the presence of diffusible and/or copper(II) bound hydroxyl radicals. This study shows that copper has a polyvalent role in the processes of tyrosine nitration.



INTRODUCTION

Biomolecule oxidation plays an important role in aging and the development of diseases. There are two major classes of intermediates involved in the *in vivo* oxidative reactions, reactive oxygen species (ROS) and reactive nitrogen species (RNS).¹ At low/moderate concentrations, ROS/RNS are important messengers for signal transduction, while at high concentrations, they can induce oxidative damage to DNA, lipids, and proteins, a phenomenon named as oxidative stress.^{2,3}

RNS can react with proteins to induce tyrosine nitration. This process is drawing considerable interest as it can alter protein functions. It can also be used as a diagnostic biomarker for diseases involving radical reactions, such as cardiovascular,⁴ Alzheimer's,⁵ and Parkinson's diseases.⁶ It is widely accepted that tyrosine nitration occurs in the presence of either peroxynitrite anion (ONOO^-)⁷ or nitrogen dioxide ($\cdot\text{NO}_2$).⁸ ONOO^- is a RNS anion generated *in vivo* by the very fast combination of nitric oxide ($\cdot\text{NO}$) and superoxide anion (O_2^-).^{9–11} $\cdot\text{NO}_2$ can be generated via several mechanisms, including the oxidation of $\cdot\text{NO}$ by oxygen,¹² the decomposition of ONOO^- ,^{7,11,13} and the oxidation of nitrite (NO_2^-) by hydrogen peroxide (H_2O_2) catalyzed with peroxidases.¹⁴ Peroxidases are often heme-containing enzymes,¹⁴ where the heme is an iron-protoporphyrin IX able to accept or donate electrons and to interconvert among the states of Fe(II), Fe(III), and Fe(IV).¹⁴

Herein, we have investigated cupric ions (Cu^{2+}) or Cu^{2+} –peptide complexes-catalyzed peptide nitration in the presence of either nitrite or nitric oxide. Copper is able to favor the generation of free radicals causing oxidative damage to proteins, lipids,

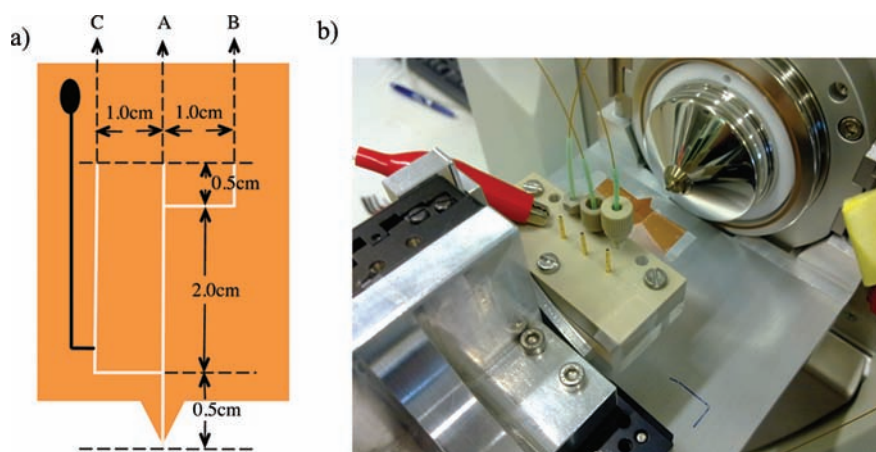
and nucleic acids.^{15,16} Copper at high concentrations can be an important factor in the pathogenesis of many neurodegenerative disorders,^{17,18} and the binding between copper and disease-associated peptides or proteins has been widely studied.^{19,20} However, Cu^{2+} -catalyzed nitration has attracted little attention, especially in mechanistic and pathogenesis studies. To date, most of the studies about copper related tyrosine nitration have focused on copper–zinc superoxide dismutase (Cu,Zn-SOD). Apart from its principal role in scavenging the superoxide anion O_2^- to form hydrogen peroxide and oxygen, it has been shown to promote the oxidation of nitrite to form nitrogen dioxide.^{21–24}

In this study, electrospray ionization (ESI) mass spectrometry (MS) was used to analyze the nitration products. Specifically, we have designed a dedicated polymer microchip reactor that also acts as an ESI emitter to monitor on-line nitrite-induced peptide nitration. Both Cu^{2+} and Cu^{2+} –peptide complexes were found to catalyze the tyrosine nitration in the presence of nitrite and hydrogen peroxide. To explain the observed copper-mediated tyrosine nitration, a mechanism was proposed where hydroxyl radicals ($\cdot\text{OH}$) and/or copper(II)-bound $\cdot\text{OH}$ (Cu^{2+} – $\cdot\text{OH}$) can be generated from Cu^{2+} and H_2O_2 through a Fenton-like reaction. These radicals may then be scavenged by both NO_2^- to form $\cdot\text{NO}_2$ and tyrosine to form tyrosine radicals (Tyr^\cdot), leading to tyrosine nitration. $\text{Cu}^{2+}/\text{H}_2\text{O}_2$ was also found to catalyze the tyrosine nitration induced by nitric oxide and oxygen. $\cdot\text{NO}$ was oxidized by O_2 to form $\cdot\text{NO}_2$, and the role of $\text{Cu}^{2+}/\text{H}_2\text{O}_2$ was to

Received: July 26, 2011

Published: November 02, 2011

Scheme 1. (a) Polyimide Microchip with Three Microchannels (White Lines) and One Micro-carbon Electrode (Black Line); and (b) the Microchip Works as an Electrospray Emitter for On-Line Tyrosine Nitration Study^a



^a The depths and widths of all microchannels are 50 and 100 μm , respectively.

generate $\cdot\text{OH}/\text{Cu}^{2+}-\cdot\text{OH}$ to promote Tyr \cdot formation. This work shows that cupric ions and peptide–cupric ion complexes are very efficient Fenton catalysts having neurotoxicity, for example, inducing nitration of α -synuclein relevant to Parkinson's disease.^{6,25}

EXPERIMENTAL SECTION

Nitration Induced by Nitrite. Off-line tyrosine nitration was performed by incubating angiotensin I (Ang I, 0.25 mM, trifluoroacetate salt), CuCl_2 (0.25 mM), H_2O_2 (0.5 mM), and NaNO_2 (1 mM) in H_2O under ambient temperature and pressure in a 1.5 mL Eppendorf tube under persistent shaking for 4 h. After reaction, the products were diluted 11 times in an ESI buffer of 50% methanol with 49% H_2O and 1% acetic acid (50%MeOH/49% H_2O /1%HAc) before MS identification. Detailed information about all chemicals used can be found in Supporting Information S-1.

On-line nitration was directly performed in a microchip as shown in Scheme 1 followed with MS identification. The microchip fabrication is illustrated in Supporting Information S-2 by using a previously reported scanning laser ablation method.^{26,27} Solution A of Ang I (0.5 mM, trifluoroacetate salt), H_2O_2 , and NaNO_2 in H_2O was pushed by a syringe pump through channel A. Solution B of Fe^{2+} , Fe^{3+} , heme, Cu^{2+} , β -amyloid 16 copper(II) complex ($\text{A}\beta$ -16- Cu^{2+}), ethylene-diaminetetraacetic acid copper(II) complex ($\text{EDTA}-\text{Cu}^{2+}$), or 1,4,8,11-tetraazacyclotetradecane copper(II) complex ($\text{TC}-\text{Cu}^{2+}$) was pushed through channel B. At the end of channel A, the ESI buffer was introduced by channel C to maintain steady ionization conditions. Nitration of Ang I occurred under ambient temperature and pressure in channel A, mostly before the introduction of the ESI buffer. By controlling the different flow rates, the reaction time in channel A can be controlled. On-line nitration of α -synuclein, leu-enkephalin, or 4-aminophenol was performed similarly just by replacing Ang I in channel A with these substrates. The $\text{A}\beta$ -16- Cu^{2+} , $\text{TC}-\text{Cu}^{2+}$, and $\text{EDTA}-\text{Cu}^{2+}$ complexes were prepared by incubating the $\text{A}\beta$ -16 peptide, TC, and EDTA with CuCl_2 , respectively, with a ratio of 2:1 (mol:mol) for 1 h under persistent shaking in ambient conditions.

Nitration Induced by Nitric Oxide. Diethylamine NONOate sodium salt hydrate (NONOate) was used to generate nitric oxide, $\cdot\text{NO}$. The nitration was performed off-line by incubating Ang I (0.25 mM, trifluoroacetate salt) with NONOate (2.5 mM of initial concentration) in water under persistent shaking at ambient temperature and pressure.

H_2O_2 and Cu^{2+} may be added to assist the nitration. To perform the reaction under anaerobic conditions, nitrogen was used to remove dissolved oxygen in water, and the reaction was performed under the protection of nitrogen. After reaction, the sample was diluted 11 times in the ESI buffer before MS identification.

Mass Spectrometry. Mass spectrometry (MS) and tandem mass spectrometry (MS/MS) experiments were performed on the Thermo LTQ Velos. For MS experiments, 3.7 kV of voltage was applied to induce electrospray ionization. For MS/MS experiments, collision-induced dissociation (CID) was performed under 20% of instrumental collision energy.

For the on-line nitration induced by nitrite, MS analyses were performed using the microchip emitter shown in Scheme 1, where a carbon electrode placed in channel C was used to supply the high-voltage. For the off-line nitration induced by nitrite, a similar microchip with a carbon electrode placed in channel A was used as an emitter. The diluted reaction product was pushed by a syringe pump through the channel A with a flow rate of 1.1 $\mu\text{L min}^{-1}$. Channels B and C were blocked during these experiments.

MS analyses of nitration induced by $\cdot\text{NO}$ were performed with the commercial ESI source. The diluted reaction products were pushed by a syringe pump at a flow rate of 10 $\mu\text{L min}^{-1}$.

All MS instrumental parameters were kept constant during experiments for the microchip ESI–MS and commercial source ESI–MS, respectively.

Characterization of Hydroxyl Radical Generation from Copper(II) and H_2O_2 . $\cdot\text{OH}/(\text{Cu}^{2+}-\cdot\text{OH})$ radicals generated from Cu^{2+} and H_2O_2 were characterized using a fluorometric assay.^{28,29} The fluorescence spectra of 2-hydroxyterephthalic acid generated by the reaction of terephthalic acid with $\cdot\text{OH}/(\text{Cu}^{2+}-\cdot\text{OH})$ were obtained on a Perkin-Elmer LS-50B fluorescence spectrometer. An aqueous solution of terephthalic acid (0.1 mM, saturated), H_2O_2 (3 mM), and CuCl_2 (3 mM) with or without NaNO_2 (3 mM) was incubated in ambient temperature and pressure before the fluorescence detection. The excitation wavelength for fluorescence detection was 315 nm, and the signal was recorded at 430 nm.

RESULTS AND DISCUSSION

On-Line Tyrosine Nitration Induced by Copper(II), Nitrite, and H_2O_2 . Copper(II) was found to catalyze tyrosine nitration in the presence of nitrite and H_2O_2 . To efficiently analyze the

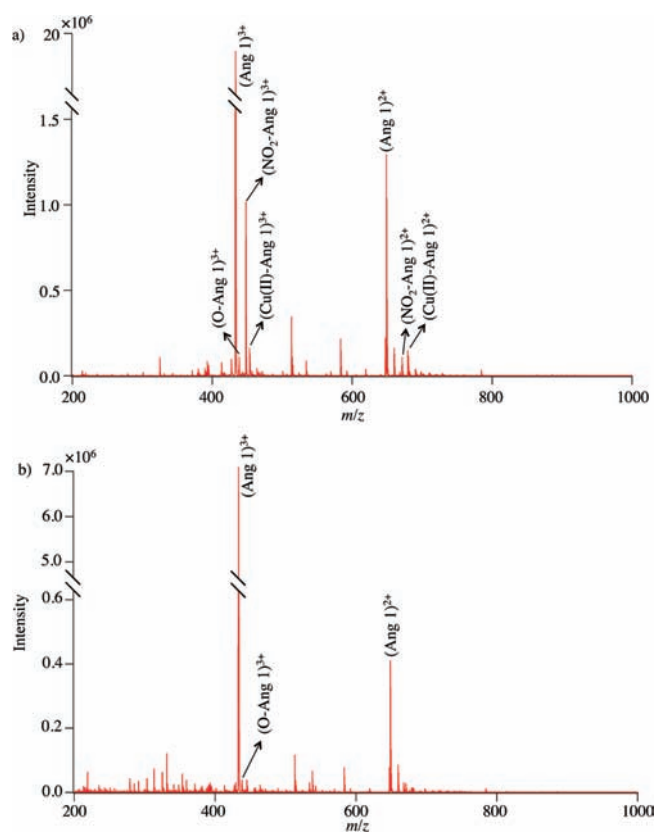


Figure 1. (a) Mass spectrum of Ang I on-line nitration products. Flow rates in channels A and B = $0.05 \mu\text{L min}^{-1}$ and in channel C = $1 \mu\text{L min}^{-1}$. Channel A, 0.5 mM of Ang I, 1 mM of H_2O_2 , and 2 mM of NaNO_2 in H_2O ; channel B, 0.5 mM of CuCl_2 in H_2O ; channel C, ESI buffer. (b) Mass spectrum obtained under the same experimental conditions as in (a) except that the solution in channel B was changed to deionized water.

nitration products, a three-channel microchip was fabricated working both as a reactor for tyrosine nitration and as an emitter for electrospray ionization, as shown in Scheme 1. Peptide solutions were pumped into channel A together with H_2O_2 and sodium nitrite (NaNO_2). Copper(II) chloride (CuCl_2) solutions were brought by channel B to react with nitrite, H_2O_2 , and peptide in the 2 cm long reaction flow channel A. At the end of the reaction channel, a large amount of ESI buffer was introduced by channel C to help sample ionization and to maintain steady ionization conditions so as to obtain a good reproducibility required for quantitative analysis. The reaction products were directly ionized and detected by a linear ion trap mass spectrometer. Angiotensin I (Ang I) was used as a test sample for the nitration study. As shown in Figure 1a, both nitrated and unmodified Ang I were detected by mass spectrometry. With tandem MS experiments, it was further demonstrated that the nitration happens always on the single tyrosine residue of Ang I (see Supporting Information S-3). Oxidized Ang I (O-Ang I) and copper(II)-binding Ang I (Cu(II)-Ang I) were also observed.

When the CuCl_2 solution in channel B was changed to pure water, the nitrated Ang I (NO_2 -Ang I) and Cu(II)-Ang I were no longer observed, while peaks of the bare and oxidized Ang I remained, as shown in Figure 1b. The details of the observed peaks are listed in Supporting Information Table S-4. It is then

clear that Ang I nitration induced by hydrogen peroxide and nitrite occurs only in the presence of Cu^{2+} . The weak peak of O-Ang I observed in both Figure 1a and b can be a result of the direct oxidation of the peptide during the electrospray process rather than oxidation induced by Cu^{2+} and H_2O_2 . Indeed, it was reported previously that the high voltage applied for ESI could result in the oxidation of samples.^{30,31} Besides angiotensin I, similar tyrosine nitration reactions were observed with leu-enkephalin or a fragment of human α -synuclein (107–140), as shown in Supporting Information Figure S-5.

On-Line Tyrosine Nitration under Various Concentrations of Copper(II), H_2O_2 , and Nitrite. Tyrosine nitration efficiencies were compared under various experimental conditions. To calculate quantitatively the nitration levels from the mass spectra, an external calibration method was employed as illustrated in Supporting Information S-6. Specifically, $M_1/(M_1 + M_2)$ was calculated from $P_1/(P_1 + P_2)$ to show the nitration level by using the calibration curves shown in Figure S-6, where M_1 is the concentration of NO_2 -Ang I produced, M_2 is the concentration of unreacted Ang I, P_1 is the monoisotopic peak intensity of three-times protonated NO_2 -Ang I (NO_2 -Ang I)³⁺ read from the mass spectra, and P_2 is the monoisotopic peak intensity of three-times protonated Ang I (Ang I)³⁺.

As shown in Supporting Information Figure S-7, the nitration can reach steady-state conditions within 1 min. Therefore, a flow rate of $0.05 \mu\text{L min}^{-1}$ for both channels A and B, corresponding to a reaction time of 1 min, was then used as the standard flow rate for the following on-line tyrosine nitration studies.

To investigate the effect of NO_2^- , its concentration was varied while maintaining the concentrations of Ang I, CuCl_2 , and H_2O_2 constant. Flow rates in all three channels were also kept constant. Zoomed mass spectra of the three-times protonated NO_2 -Ang I generated under different experimental conditions are shown in Figure 2a. Each mass spectrum shown is an average of ~ 500 spectra collected continually during 3 min. The mass spectra were normalized by always taking the intensity of the monoisotopic peak of (Ang I)³⁺ equal to 100 for comparison. The calculated nitration levels were plotted against the nitrite concentrations, as shown in the inset. The data illustrate that tyrosine nitration strongly relies on the presence of NO_2^- with an observed optimal concentration of between 1 and 2.5 mM. Interestingly, the nitration level was attenuated greatly with higher concentrations of NO_2^- .

Similarly, the influences of H_2O_2 and copper(II) on the tyrosine nitration yield were also investigated. As was observed in Figure 2b, the nitration level increases quickly when the H_2O_2 concentration increases from 0.125 to 0.5 mM, reaching a maximum for H_2O_2 concentrations above 1 mM. This indicates that nitration is then limited by other reactants. A strong copper(II)-dependent nitration is observed when the concentration of CuCl_2 increases from 12.5 μM to 0.5 mM, while the nitration yield does not vary much when the concentration of CuCl_2 increases from 0.5 to 5 mM; see Figure 2c. The highest observed nitration level of Ang I with optimized reactant concentrations is $\sim 10\%$. The nitration of Ang I induced by copper(II), nitrite, and H_2O_2 happened always under weak acidic conditions ($\text{pH} = 4.0 \pm 0.3$) due to the acidity of angiotensin I trifluoroacetate salt itself.

Off-Line Tyrosine Nitration Induced by NO/O_2 with the Catalysis of Copper(II)/ H_2O_2 . It was found that a trace amount of copper(II) can also catalyze nitration induced by NO and O_2 in the presence of H_2O_2 . Diethylamine NONOate sodium

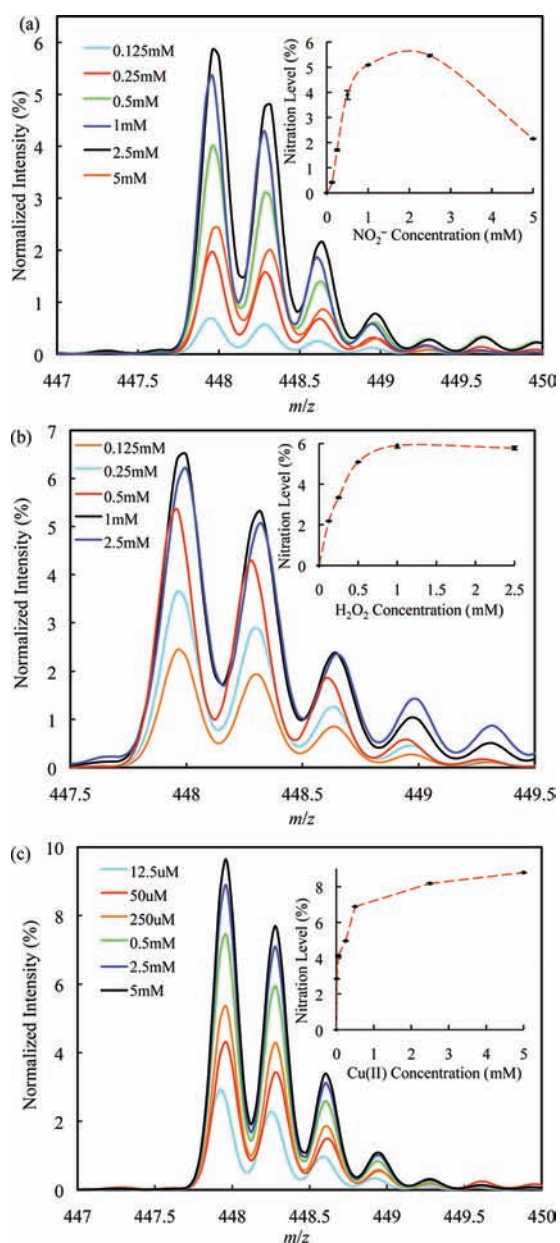


Figure 2. Ang I nitration under different concentrations of (a) NO_2^- , (b) H_2O_2 , and (c) CuCl_2 . Flow rates in channels A and B = $0.05 \mu\text{L min}^{-1}$ and in channel C = $1 \mu\text{L min}^{-1}$. Channel A, Ang I (0.5 mM), H_2O_2 , and NaNO_2 in H_2O ; channel B, CuCl_2 in H_2O ; channel C, ESI buffer. All of the concentrations shown in the figure are those of the reactants in the microreactor just after mixing solutions from channels A and B. (a) $\text{CuCl}_2 = 0.25 \text{ mM}$, $\text{H}_2\text{O}_2 = 0.5 \text{ mM}$. (b) $\text{CuCl}_2 = 0.25 \text{ mM}$, $\text{NO}_2^- = 1 \text{ mM}$. (c) $\text{H}_2\text{O}_2 = 0.5 \text{ mM}$, $\text{NO}_2^- = 1 \text{ mM}$. Mass spectra were normalized by setting the monoisotopic peak intensities of $(\text{Ang I})^{3+}$ always as 100%. Insets: Calculated nitration levels versus concentrations. The error bars show the standard deviations of the calculated nitration levels.

salt hydrate (NONOate) was used as an $\cdot\text{NO}$ generator³² to incubate with Ang I in water. Because $\cdot\text{NO}$ was generated during the decomposition of NONOate, batch reactions were carried out instead of the on-line microchip strategy to study $\cdot\text{NO}$ -induced nitration. After 4 h of reaction in water, the nitration products were analyzed by MS using the commercial ESI source.

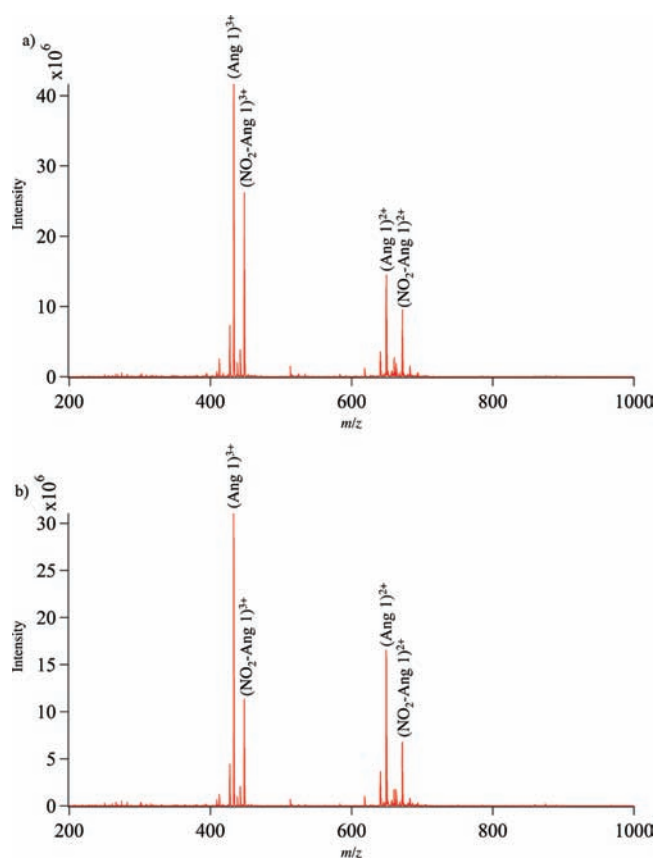


Figure 3. NONOate (2.5 mM)/ O_2 -induced Ang I (0.25 mM) nitration in water (a) with or (b) without H_2O_2 (1 mM) and CuCl_2 (12.5 μM) after 4 h of reaction. The products were diluted 11 times in the ESI buffer and then analyzed by ESI-MS with a flow rate of $10 \mu\text{L min}^{-1}$.

As is shown in Figure 3b, strong nitration of Ang I can be observed. However, a more efficient nitration was obtained when H_2O_2 and a trace amount of Cu^{2+} (12.5 μM) were added into the above reaction system, Figure 3a.

A quantitative analysis was performed with the external calibration method given in Supporting Information S-6. The nitration levels of Ang I achieved under various reactant conditions were systematically compared in Figure 4. As shown in Figure 4b, oxygen is necessary for $\cdot\text{NO}$ -induced nitration. Only background levels of nitration were observed when the reaction was performed under a nitrogen-protected environment. The nitration induced by $\cdot\text{NO}/\text{O}_2$ can be significantly catalyzed only in the presence of H_2O_2 and trace amounts of copper(II), while high concentrations of copper(II) would inhibit the $\cdot\text{NO}/\text{O}_2$ -induced nitration.

Figure 4a compares the nitration levels that were obtained under trace and large amounts of copper(II) for various reaction times. The nitration catalyzed by 12.5 μM of copper(II) is very fast and reaches a steady state within 1 h, while in the presence of 2.5 mM of copper(II) it reaches steady state after 7 h of incubation. Nitration under various concentrations of copper(II) was further investigated. As shown in Figure 4c, the nitration level decreases with the increase of copper(II) concentration. When the Cu^{2+} concentration is higher than 0.5 mM, nitration induced by $\cdot\text{NO}/\text{O}_2$ without copper(II) is even more efficient than that with copper(II). The influence of H_2O_2 on $\cdot\text{NO}/\text{O}_2$ -induced nitration catalyzed by a trace amount of Cu^{2+} was also studied. As shown in Figure 4d, the nitration level always

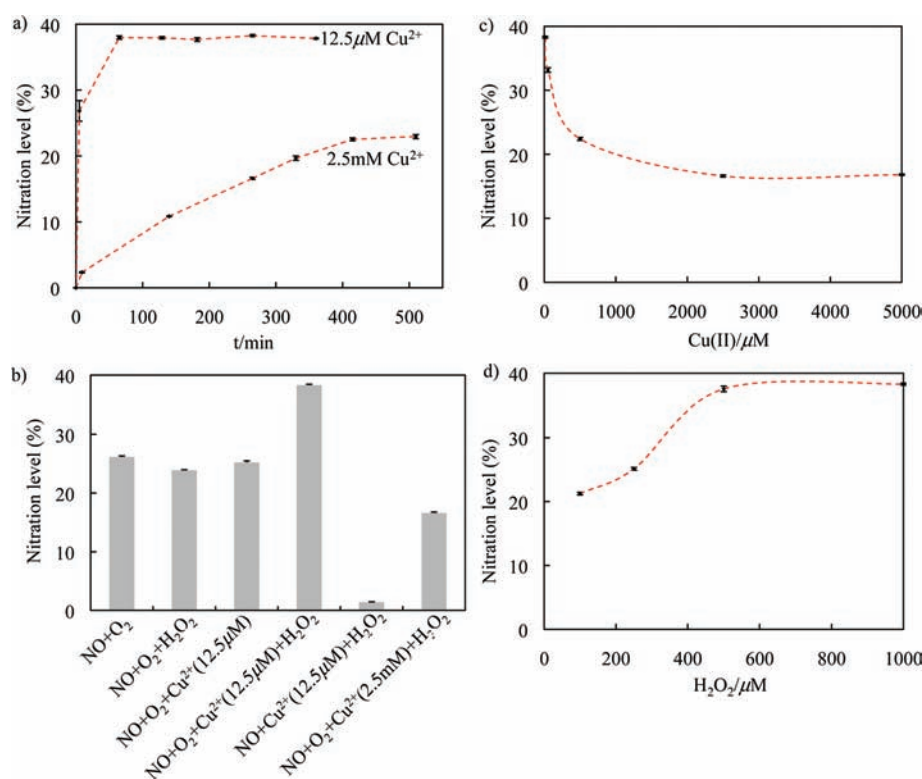


Figure 4. (a) NONOate (2.5 mM)/O₂-induced Ang I nitration in water with H₂O₂ (1 mM) and CuCl₂ (12.5 μM or 2.5 mM) under various reaction times. (b) NONOate (2.5 mM)/O₂-induced Ang I nitration in water under various reactant conditions after 4 h of reaction. The concentration of H₂O₂ was always 1 mM. (c) NONOate (2.5 mM)/O₂ induced Ang I nitration in water with H₂O₂ (1 mM) and various amounts of CuCl₂ after 4 h of reaction. (d) NONOate (2.5 mM)/O₂-induced Ang I nitration in water with CuCl₂ (12.5 μM) and various amounts of H₂O₂ after 4 h of reaction. The error bars show the standard deviations of the calculated nitration levels.

increases with the increase of H₂O₂ concentration. The acidity of angiotensin I trifluoroacetate salt was neutralized by the basic NONOate. As a result, the nitration of Ang I induced by [•]NO/O₂ happened always under neutral conditions (pH = 7.5 ± 0.2).

Role of Copper(II) in Nitrating Tyrosine. Tyrosine nitration can occur via several mechanisms originating either from nitric oxide ([•]NO) or from nitrite (NO₂⁻).

The [•]NO pathways involve its oxidation by oxygen to form ultimately nitrogen dioxide ([•]NO₂),¹² which is the key nitrating agent. [•]NO can also react with superoxide anions (O₂⁻) to form peroxyntirite (ONOO⁻) that may decompose, depending on the biological conditions, to form nitronium ion (NO₂⁺)^{33–35} or [•]NO₂.^{7,11,13} In the presence of CO₂, ONOOCO₂⁻ can be generated from ONOO⁻, and further decomposes into carbonate radicals and [•]NO₂ to induce tyrosine nitration.^{7,11}

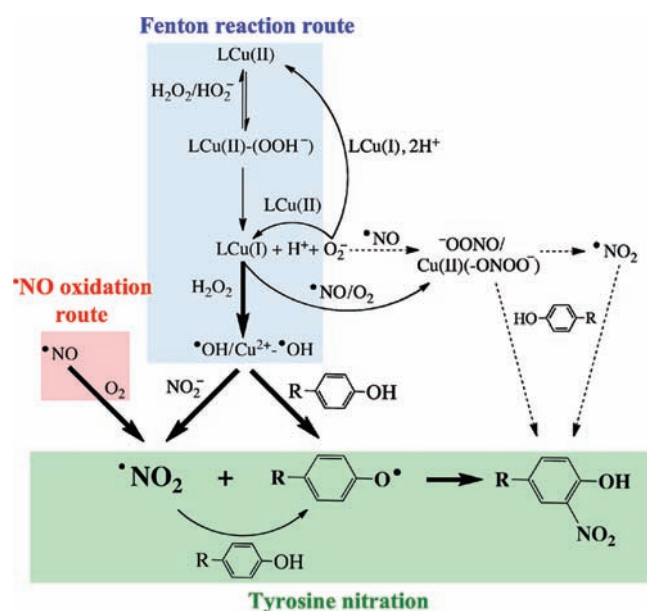
The nitrite (NO₂⁻) pathways are usually considered to be enzymatically driven where NO₂⁻ is oxidized in the presence of H₂O₂ and peroxidase to form nitrogen dioxide ([•]NO₂).^{14,36} Alternatively, enzyme–ONOO⁻ complexes can also be generated from peroxidases, H₂O₂, and NO₂⁻ to react directly with tyrosine and induce nitration.³⁷

Beside peroxidases, heme, heme-containing proteins, such as myoglobin and cytochrome *c*, and Fe²⁺/Fe³⁺ can also catalyze nitration through mechanisms similar to those involving peroxidases.^{14,38,39} The heme–protein/H₂O₂/NO₂⁻ facilitated nitration and the chemical biology of ONOO⁻ have been extensively reviewed in recent publications.^{9,36,40–42}

In comparison to the well-established mechanisms for peroxidase, heme, and iron-induced tyrosine nitration, the role of

copper is less known in protein nitration. According to previous studies, copper(II) is able to catalyze the decomposition of peroxyntirite to oxidize special substrates, such as ascorbic acid, or to induce nitration.^{43–46} Alternatively, peroxyntirite coordinated copper(II), which is generated in the presence of copper(I) complexes, [•]NO, and O₂, can undergo further decomposition inducing tyrosine nitration.^{47–49} The nitrite related tyrosine nitration was reported to be induced by copper–zinc superoxide dismutase (SOD) via Fenton reactions¹⁴ in the presence of hydrogen peroxide.^{21–24} Indeed, Cu²⁺ in SOD is assumed to be reduced to copper(I) by H₂O₂ that in turn can react with H₂O₂ via a Fenton-like reaction to generate copper(II)-bound [•]OH (Cu²⁺–[•]OH) that oxidizes nitrite to nitrogen dioxide.

On the basis of the enzymatic redox mechanisms,^{21–24} a pathway for the present copper(II)-induced nitration by nitrite is proposed as shown in Scheme 2. In the presence of H₂O₂/HO₂⁻, copper(II) can be coordinated by hydroperoxide anion (HO₂⁻) to form a key complex of copper(II)–hydroperoxo. The complex can further decompose to generate copper(I) to react with H₂O₂ via a Fenton-like reaction to produce [•]OH and/or Cu²⁺–[•]OH, as highlighted to be the Fenton reaction route shown in Scheme 2. The [•]OH/Cu²⁺–[•]OH radicals contribute to both the generation of [•]NO₂ in the presence of nitrite and the production of Tyr[•] from tyrosine, leading to the nitration of tyrosine. With this mechanism, the on-line nitrite-induced nitration should happen mainly in aqueous channel A before the addition of the ESI buffer. This is because methanol in this buffer is a scavenger of hydroxyl radicals thereby terminating the radical reactions.⁵⁰ Considering the pH conditions used in the experiments,

Scheme 2. Proposed Mechanism for Copper(II) and Peptide–Copper(II)-Induced Tyrosine Nitration^a

^a L: ligand.

H_2O_2 ($\text{pK}_a = 11.6$) should be the main species to react with cupric ions in the case of copper(II), nitrite, and H_2O_2 -induced Ang I nitration ($\text{pH} = 4.0 \pm 0.3$). In theory, more HO_2^- could participate in the reaction in the case of $\cdot\text{NO}/\text{O}_2$ induced Ang I nitration ($\text{pH} = 7.5 \pm 0.2$), leading to an increased reaction rate to produce $\cdot\text{OH}$.

To validate the proposed mechanism, fluorometric experiments were carried out using terephthalic acid to characterize the generation of $\cdot\text{OH}$ radicals.^{28,29} Terephthalic acid has been used in the past as a highly specific and sensitive hydroxyl radical dosimeter in radiation chemistry and sonochemistry.^{51,52} In the presence of $\cdot\text{OH}$, 2-hydroxyterephthalic acid is generated, yielding a strong fluorescence signal at 430 nm under UV light irradiation at 315 nm. It was proven that other radicals, such as $\cdot\text{OOH}$ and O_2^- , cannot directly induce a similar fluorescence.⁵³ As shown in Figure 5 and Supporting Information Figure S-8, fluorescence was observed from the reaction products of H_2O_2 , CuCl_2 , and terephthalic acid, rising linearly with the reaction time, indicating the abundant generation of $\cdot\text{OH}$ from H_2O_2 and CuCl_2 . When NaNO_2 was added, the production of 2-hydroxyterephthalic acid decreased, illustrating that NO_2^- competed for $\cdot\text{OH}$ quenching to form $\cdot\text{NO}_2$. All of the fluorometric experiments were performed under weak acidic conditions ($\text{pH} = 4.2 \pm 0.1$) due to the acidity of terephthalic acid, in accordance with the nitration induced by copper(II), nitrite, and H_2O_2 . It is calculated that $\sim 70\%$ of $\cdot\text{OH}$ generated is scavenged by NO_2^- under the experimental conditions in the presence of nitrite, and that the rate constant for $\cdot\text{OH}$ scavenging by nitrite is 8% that of terephthalic acid. Thus, this shows that nitrite is a rather efficient $\cdot\text{OH}$ scavenger but is not as efficient as terephthalic acid; see Supporting Information S-8. According to the mechanism proposed for nitration induced by SOD, an oxidant of SOD– Cu^{2+} – $\cdot\text{OH}$ is generated instead of diffusible $\cdot\text{OH}$.²² Similarly, the copper(II)-bound hydroxyl radical may also be generated in this mechanism, perhaps exhibiting chemical properties similar to those of diffusible $\cdot\text{OH}$ to induce the fluorescence. Therefore, the

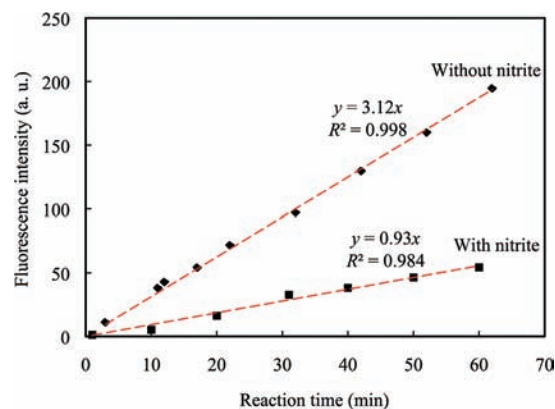


Figure 5. Characterization of $\cdot\text{OH}$ radical production from H_2O_2 (3 mM) and copper(II) (3 mM) with or without nitrite (3 mM): fluorescence intensity (430 nm) versus reaction time plot. Baselines were subtracted from the spectra to calculate the fluorescence intensities. Unmodified fluorescence spectra are shown in Figure S-8.

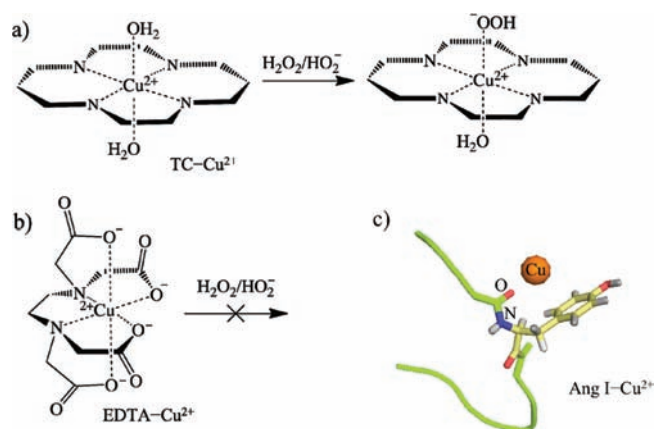
characterized $\cdot\text{OH}$ by terephthalic acid can be a sum of both diffusible and copper(II)-bound hydroxyl radicals.

According to the fluorometric results in Figure 5, $\cdot\text{OH}$ and/or Cu^{2+} – $\cdot\text{OH}$ can be generated from H_2O_2 and copper(II) and further scavenged by nitrite to form possibly $\cdot\text{NO}_2$. This sequence is in accordance with the proposed Fenton reaction route in Scheme 2. Another important reactant that can mediate tyrosine nitration is peroxynitrite. Although it was reported that enzyme-bound peroxynitrite can be formed from nitrite and H_2O_2 in the presence of peroxidases or heme containing proteins,^{37–39} copper(II) was reported to catalyze peroxynitrite decomposition.⁴⁴ Therefore, the peroxynitrite is not likely to be generated from nitrite and H_2O_2 under our experimental conditions, and the $\cdot\text{NO}_2$ -mediated nitration is more likely to be the main reaction route of the nitrite-induced nitration.

The results of nitration occurring under various concentrations of H_2O_2 and NO_2^- shown in Figure 2 also support the proposed mechanism in Scheme 2. A large amount of $\cdot\text{OH}$ can be generated with concentrated H_2O_2 , which would favor the nitration of tyrosine, in accordance with Figure 2b. The ratio between $\cdot\text{OH}$ and NO_2^- in the reaction system is an important factor. With an excess amount of NO_2^- , all $\cdot\text{OH}$ radicals would be scavenged by nitrite. Therefore, Tyr^\bullet can only be produced from the reaction between $\cdot\text{NO}_2$ and tyrosine, leading to limited nitration, in agreement with Figure 2a.

In the presence of $\cdot\text{NO}$, several pathways are possible to induce tyrosine nitration by considering the copper(II) redox mechanisms shown in Scheme 2. Because O_2^- is produced during the decomposition of H_2O_2 catalyzed by copper(II), ONOO^- may be generated from the combination of $\cdot\text{NO}$ and O_2^- to induce tyrosine nitration. However, O_2^- can also be removed by the excess of copper(II)/copper(I) efficiently,^{54,55} resulting in the ONOO^- route being less feasible. Alternatively, $\cdot\text{NO}_2$ can be generated by oxidizing $\cdot\text{NO}$ with O_2 to induce nitration.¹² Considering the observation that $\cdot\text{NO}$ -induced tyrosine nitration occurs only in the presence of oxygen and that copper(II) is not essential for the $\cdot\text{NO}$ induced nitration, the $\cdot\text{NO}$ oxidation route highlighted in Scheme 2 is the most likely under the present conditions. In the presence of $\text{Cu}^{2+}/\text{H}_2\text{O}_2$, production of Tyr^\bullet is promoted by the production of $\cdot\text{OH}/\text{Cu}^{2+}$ – $\cdot\text{OH}$ radicals, and therefore more efficient nitration was observed

Scheme 3. Structures of the TC–Cu²⁺, EDTA–Cu²⁺, and Ang I–Cu²⁺ Complexes



as shown in Figures 3 and 4. In addition, it is possible to generate peroxynitrite or copper(II) bound peroxynitrite from $\cdot\text{NO}$, O_2 , and copper(I) complexes to induce nitration.^{47–49} However, abundant copper(II) inhibits nitration induced by $\cdot\text{NO}$, possibly because a large amount of copper(II) can scavenge the $\cdot\text{NO}$ by forming a $\text{NO}-\text{Cu}^{2+}(\text{L})$ complex, where L is any ligand.⁵⁶

Coordinated Copper(II) as Fenton Catalyst. Copper can be easily coordinated by various ligands. The copper(II)/copper(I) complexes were also reported to catalyze peroxynitrite decomposition to induce ascorbic acid oxidation and nitration, and to catalyze the formation of peroxynitrite coordinated copper(II) from $\cdot\text{NO}$ and O_2 .^{43,47,57} Copper complexes that hold SOD-like properties, peroxidase properties, and antioxidant properties have already been synthesized.^{58,59}

In Figure 1a, the peaks of Ang I monocoordinated copper(II) are observed, demonstrating the presence of Ang I–Cu²⁺ during the Ang I nitration. According to the tandem MS results shown in Supporting Information S-9, Cu²⁺ should bind to the carbonyl group on the backbone between valine and tyrosine, in accordance with the literature.⁶⁰ The structure of Ang I–Cu²⁺ is shown in Scheme 3. Because it has been reported that amino acid monocoordinated Cu²⁺ shows enhanced activity for the decomposition of H_2O_2 ,⁶¹ it can be proposed that both peptide-coordinated and noncoordinated Cu²⁺ may play a role in the copper-catalyzed tyrosine nitration.

To study if Cu²⁺ can catalyze nitration without peptides, 4-aminophenol (AP) was used as a substrate for a nitrite-induced nitration. In the presence of Cu²⁺, nitrite, and H_2O_2 , nitrated AP was generated together with the oxidized AP and detected by mass spectrometry. This illustrates that copper(II) itself is a good Fenton catalyst, Supporting Information S-10.

To evaluate the performance of coordinated copper(II) in tyrosine nitration, different copper(II) complexes were prepared, including β -amyloid-16 peptide coordinated copper(II) (A β -16–Cu²⁺), 1,4,8,11-tetraazacyclotetradecane coordinated copper(II) (TC–Cu²⁺), and ethylenediaminetetraacetic acid coordinated copper(II) (EDTA–Cu²⁺). When TC–Cu²⁺ was used instead of uncoordinated Cu²⁺ to catalyze the nitration of Ang I, nitrite-induced tyrosine nitration was still realized. The nitration level observed was similar to that when uncoordinated Cu²⁺ was employed; see Figure 6. The affinity between TC and Cu²⁺ is very strong; thus, no free Cu²⁺ or peptide coordinated Cu²⁺ can take part in the nitration of tyrosine when an excess of TC is used.

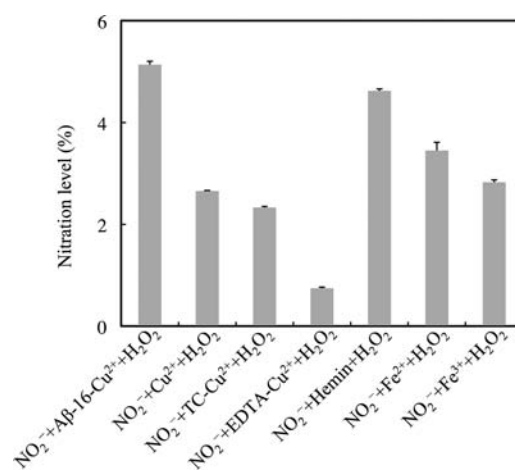


Figure 6. Ang I on-line nitration catalyzed by different metal ions. Flow rates in channels A and B = 0.05 $\mu\text{L min}^{-1}$ and in channel C = 1 $\mu\text{L min}^{-1}$. Channel A, 0.5 mM of Ang I, 1 mM of H_2O_2 , and 2 mM of NaNO_2 in H_2O ; channel B, 25 μM of A β -16–Cu²⁺, Cu²⁺, TC–Cu²⁺, EDTA–Cu²⁺, heme, Fe²⁺, or Fe³⁺ in H_2O ; channel C, ESI buffer. The error bars show the standard deviations of the calculated nitration levels. The concentrations of different metal ions were all 25 μM because the maximum concentration of heme in water under ambient conditions is 25 μM .

As shown in Scheme 3, the hydroperoxide anion should therefore coordinate TC–Cu²⁺ as an axial ligand to form the key complex of copper(II)–hydroperoxo. The complex can further decompose to generate TC–copper(I) complex. When EDTA–Cu²⁺ was used, only a background level of nitrite-induced tyrosine nitration was observed. This phenomenon supports the proposed mechanism shown in Scheme 2. In the very stable structure of EDTA–Cu²⁺, Cu²⁺ is 6-fold coordinated, and therefore the key copper(II)–hydroperoxo complex necessary for inducing copper(II) reduction cannot be generated, as shown in Scheme 3.

A β -16–Cu²⁺ was also employed instead of free copper(II) to catalyze the Ang I nitration in the presence of H_2O_2 and nitrite. A β -16 has been reported to have a strong affinity to coordinate copper(II),^{62–64} and to further control the redox activity of Cu²⁺/Cu⁺.^{65,66} As shown in Figure 6, A β -16–Cu²⁺ is a better nitration catalyst than free Cu²⁺ under the same experimental conditions, illustrating that A β -16–Cu²⁺ is a stronger Fenton catalyst.

Additionally, because proteins/peptides are able to bind various free metal ions, the abilities of different metal ions to catalyze nitration with H_2O_2 and NO_2^- were examined. Specifically, Fe²⁺, Fe³⁺, and heme were used for comparison. As shown in Figure 6, the Cu²⁺-induced nitration is almost as efficient as that mediated by Fe³⁺. An increase in efficiency of the A β -16–Cu²⁺-induced nitration, in comparison to that catalyzed by heme under the same experimental conditions, implies that Cu²⁺ or peptide-coordinated Cu²⁺ may play an important role in many neurodegenerative disorders related to tyrosine nitration.

CONCLUSION

A mass spectrometry-based methodology has been developed to study the on-line nitration of tyrosine by nitrite and hydrogen peroxide. We have demonstrated that cupric ions and cupric–peptides complexes act as efficient Fenton catalysts able

to catalyze this reaction even better than heme. This chemical pathway is similar to the enzymatic pathways classically considered. Using an off-line approach, we have shown that cupric ions in the presence of hydrogen peroxide can promote tyrosine nitration through promotion of the production of tyrosine radicals by nitric oxide. This study shows that cupric ions play a polyvalent role as Fenton catalysts to efficiently catalyze the production of $\cdot\text{OH}/\text{Cu}^{2+} - \cdot\text{OH}$ radicals. The radicals are themselves involved in many reactions. The major conclusion of this work is that micromolar concentrations of copper catalyze the nitration process by $\cdot\text{NO}$ oxidation, while millimolar concentrations catalyze the nitration process by nitrite oxidation.

■ ASSOCIATED CONTENT

S Supporting Information. Chemicals employed, microchip fabrication, tandem MS characterization of various peptides, nitration of different peptides, calibration curve for nitration level quantification, and details about the characterization of hydroxyl radical generated from copper(II) and H_2O_2 . This material is available free of charge via the Internet at <http://pubs.acs.org>.

■ AUTHOR INFORMATION

Corresponding Author

hubert.girault@epfl.ch

■ ACKNOWLEDGMENT

We thank the Swiss National Science Foundation for supporting the project “Analytical tools for proteome analysis and redoxomics (200020-127142)” and NSFC 20925517. B.L. is grateful to EPFL for a visiting professor fellowship. We thank Laboratoire de neurobiologie moléculaire et neuroprotéomique of Ecole Polytechnique Fédérale de Lausanne for the synthesis of human α -synuclein (107-140) peptide.

■ REFERENCES

- Wiseman, H.; Halliwell, B. *Biochem. J.* **1996**, *313*, 17–29.
- Apel, K.; Hirt, H. *Annu. Rev. Plant Biol.* **2004**, *55*, 373–399.
- Radi, R. *Proc. Natl. Acad. Sci. U.S.A.* **2004**, *101*, 4003–4008.
- Shishehbor, M. H.; Aviles, R. J.; Brennan, M. L.; Fu, X. M.; Goormastic, M.; Pearce, G. L.; Gokce, N.; Keaney, J. F.; Penn, M. S.; Sprecher, D. L.; Vita, J. A.; Hazen, S. L. *JAMA, J. Am. Med. Assoc.* **2003**, *289*, 1675–1680.
- Good, P. F.; Werner, P.; Hsu, A.; Olanow, C. W.; Perl, D. P. *Am. J. Pathol.* **1996**, *149*, 21–28.
- Danielson, S. R.; Held, J. M.; Schilling, B.; Oo, M.; Gibson, B. W.; Andersen, J. K. *Anal. Chem.* **2009**, *81*, 7823–7828.
- Gunaydin, H.; Houk, K. N. *Chem. Res. Toxicol.* **2009**, *22*, 894–898.
- van der Vliet, A.; Eiserich, J. P.; Halliwell, B.; Cross, C. E. *J. Biol. Chem.* **1997**, *272*, 7617–7625.
- Goldstein, S.; Lind, J.; Merenyi, G. *Chem. Rev. (Washington, DC, U. S.)* **2005**, *105*, 2457–2470.
- Schopfer, M. P.; Wang, J.; Karlin, K. D. *Inorg. Chem.* **2010**, *49*, 6267–6282.
- Surmeli, N. B.; Litterman, N. K.; Miller, A. F.; Groves, J. T. *J. Am. Chem. Soc.* **2010**, *132*, 17174–17185.
- Olbregts, J. *Int. J. Chem. Kinet.* **1985**, *17*, 835–848.
- Su, J.; Groves, J. T. *J. Am. Chem. Soc.* **2009**, *131*, 12979–12988.
- Bian, K.; Gao, Z. H.; Weisbrodt, N.; Murad, F. *Proc. Natl. Acad. Sci. U.S.A.* **2003**, *100*, 5712–5717.
- Reddy, P. V. B.; Rao, K. V. R.; Norenberg, M. D. *Lab. Invest.* **2008**, *88*, 816–830.
- Thomas, D. D.; Espey, M. G.; Vitek, M. P.; Miranda, K. M.; Wink, D. A. *Proc. Natl. Acad. Sci. U.S.A.* **2002**, *99*, 12691–12696.
- Perry, G.; Sayre, L. M.; Atwood, C. S.; Castellani, R. J.; Cash, A. D.; Rottkamp, C. A.; Smith, M. A. *CNS Drugs* **2002**, *16*, 339–352.
- Waggoner, D. J.; Bartnikas, T. B.; Gitlin, J. D. *Neurobiol. Dis.* **1999**, *6*, 221–230.
- Gaggelli, E.; Kozlowski, H.; Valensin, D.; Valensin, G. *Chem. Rev. (Washington, DC, U. S.)* **2006**, *106*, 1995–2044.
- Lu, Y.; Prudent, M.; Qiao, L. A.; Mendez, M. A.; Girault, H. H. *Metallomics* **2010**, *2*, 474–479.
- Goss, S. P. A.; Singh, R. J.; Kalyanaraman, B. *J. Biol. Chem.* **1999**, *274*, 28233–28239.
- Singh, R. J.; Goss, S. P. A.; Joseph, J.; Kalyanaraman, B. *Proc. Natl. Acad. Sci. U.S.A.* **1998**, *95*, 12912–12917.
- Zhang, H.; Joseph, J.; Felix, C.; Kalyanaraman, B. *J. Biol. Chem.* **2000**, *275*, 14038–14045.
- Bonini, M. G.; Fernandes, D. C.; Augusto, O. *Biochemistry* **2004**, *43*, 344–351.
- Sevcik, E.; Trexler, A. J.; Dunn, J. M.; Rhoades, E. *J. Am. Chem. Soc.* **2011**, *133*, 7152–7158.
- Gobry, V.; van Oostrum, J.; Martinelli, M.; Rohner, T. C.; Reymond, F.; Rossier, J. S.; Girault, H. H. *Proteomics* **2002**, *2*, 405–412.
- Bindila, L.; Froesch, M.; Lions, N.; Vukelic, Z.; Rossier, J. S.; Girault, H. H.; Peter-Katalinic, J.; Zamfir, A. D. *Rapid Commun. Mass Spectrom.* **2004**, *18*, 2913–2920.
- Ishibashi, K.; Fujishima, A.; Watanabe, T.; Hashimoto, K. *Electrochem. Commun.* **2000**, *2*, 207–210.
- Liu, J. F.; Roussel, C.; Lagger, G.; Tacchini, P.; Girault, H. H. *Anal. Chem.* **2005**, *77*, 7687–7694.
- Morand, K.; Talbo, G.; Mann, M. *Rapid Commun. Mass Spectrom.* **1993**, *7*, 738–743.
- Boys, B. L.; Kuprowski, M. C.; Noel, J. J.; Konermann, L. *Anal. Chem.* **2009**, *81*, 4027–4034.
- Maragos, C. M.; Morley, D.; Wink, D. A.; Dunams, T. M.; Saavedra, J. E.; Hoffman, A.; Bove, A. A.; Isaac, L.; Hrabie, J. A.; Keefer, L. K. *J. Med. Chem.* **1991**, *34*, 3242–3247.
- Beckman, J. S.; Carson, M.; Smith, C. D.; Koppenol, W. H. *Nature* **1993**, *364*, 584–584.
- Beckman, J. S.; Ischiropoulos, H.; Zhu, L.; Vanderwoerd, M.; Smith, C.; Chen, J.; Harrison, J.; Martin, J. C.; Tsai, M. *Arch. Biochem. Biophys.* **1992**, *298*, 438–445.
- Ramezani, M. S.; Padmaja, S.; Koppenol, W. H. *Chem. Res. Toxicol.* **1996**, *9*, 232–240.
- Roncone, R.; Barbieri, M.; Monzani, E.; Casella, L. *Coord. Chem. Rev.* **2006**, *250*, 1286–1293.
- Monzani, E.; Roncone, R.; Galliano, M.; Koppenol, W. H.; Casella, L. *Eur. J. Biochem.* **2004**, *271*, 895–906.
- Nicolis, S.; Pennati, A.; Perani, E.; Monzani, E.; Sanangelantoni, A. M.; Casella, L. *Chem.-Eur. J.* **2006**, *12*, 749–757.
- Nicolis, S.; Monzani, E.; Roncone, R.; Gianelli, L.; Casella, L. *Chem.-Eur. J.* **2004**, *10*, 2281–2290.
- Ferrer-Sueta, G.; Radi, R. *ACS Chem. Biol.* **2009**, *4*, 161–177.
- Yamakura, F.; Ikeda, K. *Nitric Oxide* **2006**, *14*, 152–161.
- Augusto, O.; Bonini, M. G.; Amanso, A. M.; Linares, E.; Santos, C. C. X.; De Menezes, S. L. *Free Radical Biol. Med.* **2002**, *32*, 841–859.
- Ferrer-Sueta, G.; Ruiz-Ramirez, L.; Radi, R. *Chem. Res. Toxicol.* **1997**, *10*, 1338–1344.
- Kohnen, S.; Halusiak, E.; Mouithys-Mickalad, A.; Deby-Dupont, G.; Deby, C.; Hans, P.; Lamy, M.; Noels, A. F. *Nitric Oxide* **2005**, *12*, 252–260.
- Babich, O. A.; Gould, E. S. *Res. Chem. Intermed.* **2002**, *28*, 575–583.
- Geletti, Y. V.; Bailey, A. J.; Boring, E. A.; Hill, C. L. *Chem. Commun. (Cambridge, U. K.)* **2001**, 1484–1485.
- Park, G. Y.; Deepalatha, S.; Puii, S. C.; Lee, D.-H.; Mondal, B.; Sarjeant, A. A. N.; del Rio, D.; Pau, M. Y. M.; Solomon, E. I.; Karlin, K. D. *J. Biol. Inorg. Chem.* **2009**, *14*, 1301–1311.

- (48) Liochev, S. I.; Fridovich, I. *J. Biol. Chem.* **2001**, *276*, 35253–35257.
- (49) Maiti, D.; Lee, D.-H.; Sarjeant, A. A. N.; Pau, M. Y. M.; Solomon, E. I.; Gaoutchenova, K.; Sundermeyer, J.; Karlin, K. D. *J. Am. Chem. Soc.* **2008**, *130*, 6700–+.
- (50) Hess, W. P.; Tully, F. P. *J. Phys. Chem.* **1989**, *93*, 1944–1947.
- (51) Price, G. J.; Lenz, E. J. *Ultrasonics* **1993**, *31*, 451–456.
- (52) Matthews, R. W. *Radiat. Res.* **1980**, *83*, 27–41.
- (53) Barreto, J. C.; Smith, G. S.; Strobel, N. H. P.; McQuillin, P. A.; Miller, T. A. *Life Sci.* **1994**, *56*, PL89–PL96.
- (54) Klugroth, D.; Rabani, J. *J. Phys. Chem.* **1976**, *80*, 588–591.
- (55) Oyoung, C. L.; Lippard, S. J. *J. Am. Chem. Soc.* **1980**, *102*, 4920–4924.
- (56) Tran, D.; Skelton, B. W.; White, A. H.; Laverman, L. E.; Ford, P. C. *Inorg. Chem.* **1998**, *37*, 2505–2511.
- (57) Geletii, Y. V.; Patel, A. D.; Hill, C. L.; Casella, L.; Monzani, E. *React. Kinet. Catal. Lett.* **2002**, *77*, 277–285.
- (58) Schepetkin, I.; Potapov, A.; Khlebnikov, A.; Korotkova, E.; Lukina, A.; Malovichko, G.; Kirpotina, L.; Quinn, M. T. *J. Biol. Inorg. Chem.* **2006**, *11*, 499–513.
- (59) Pelli, M.; Lobbia, G. G.; Santini, C.; Spagna, R.; Camalli, M.; Fedeli, D.; Falcioni, G. *Dalton Trans.* **2004**, 2822–2828.
- (60) Kim, J. Y.; Kim, M. J.; Kim, H. T. *Bull. Korean Chem. Soc.* **2010**, *31*, 1377–1380.
- (61) Lin, T. Y.; Wu, C. H. *J. Catal.* **2005**, *232*, 117–126.
- (62) Kowalik-Jankowska, T.; Ruta, M.; Wisniewska, K.; Lankiewicz, L. *J. Inorg. Biochem.* **2003**, *95*, 270–282.
- (63) Furlan, S.; Hureau, C.; Faller, P.; La Penna, G. *J. Phys. Chem. B* **2010**, *114*, 15119–15133.
- (64) Pedersen, J. T.; Teilum, K.; Heegaard, N. H. H.; Ostergaard, J.; Adolph, H. W.; Hemmingsen, L. *Angew. Chem., Int. Ed.* **2011**, *50*, 2532–2535.
- (65) Nakamura, M.; Shishido, N.; Nunomura, A.; Smith, M. A.; Perry, G.; Hayashi, Y.; Nakayama, K.; Hayashi, T. *Biochemistry* **2007**, *46*, 12737–12743.
- (66) Jiang, D.; Men, L.; Wang, J.; Zhang, Y.; Chickenyen, S.; Wang, Y.; Zhou, F. *Biochemistry* **2007**, *46*, 9270–9282.